Seeing and Manipulating Spin-Spin Interactions at the Single Atomic Level

Donghun Lee[*]

Introduction

Living in a century of digital and information world, human owe the convenient life to the two modern technologies; magnetic read sensors in hard disk drives and digital microprocessors in computers. The growing demand for more data storage, smaller size, and faster devices, however, requires a new paradigm for future electronics, 'spintronics'. In contrast to conventional charge-based electronics, spintronics relies on the electron's spin, which is a fundamental magnetic moment that has two energy states, spin-up or spin-down, analogous to the 1 or 0 states of a bit in a computer. One key challenge for the realization of spintronics is the development of ferromagnetic semiconductors which could potentially combine the advantages of magnetic recording and digital logic in a single device.

One promising candidate of ferromagnetic semiconductors is GaMnAs, in which nonmagnetic GaAs can be made ferromagnetic by introducing only a few percent of Mn. Since its discovery in 1996[1], GaMnAs has been attracting lots of interests among researchers not only because it is based on the technically important GaAs semiconductor, but also because it shows physically interesting long range magnetic interactions and it has capabilities of optical and electrical manipulation of its magnetic properties[2,3]. Nevertheless, some important challenges such as its low ferromagnetic transition temperature (currently $T_c < -100^{\circ}C$) prevent use in practical devices which operate at room temperature[4]. A better understanding of GaMnAs at a microscopic level is therefore necessary to probe the limits of T_c in this material.

In this paper, we try to answer some of the questions with atomic-scale studies by using a home-built scanning tunneling microscope. These studies are expected to give a detailed picture of magnetism in GaMnAs and contribute to a microscopic understanding of the underlying physics. Furthermore, this work will help in the search for new semiconductor materials which exhibit ferromagnetism above room temperature.

Experimental Method: Scanning Tunneling Microscope

Principles of operation; imaging, manipulation and spectroscopy

The experimental method used in this study is a scanning tunneling microscope (STM) which is one of the most advanced modern microscopes with the highest spatial resolution. The magnification is so extreme that individual atoms become visible. The heart of STM is a sharp metal needle, called a tip, placed about 1nm (1nm=10^{-9} m) away from a conducting sample surface such as a metal or semiconductor. With this proximity, once a bias voltage is applied to the tip and sample junction, electrons can overcome the energy barrier of vacuum gap, and tunnel from tip to sample or vice versa depending on the polarity of the applied bias voltage (Fig. 1a) By scanning the tip along the sample surface and monitoring the tunneling current, one can resolve the surface topography directly underneath the tip (Fig.1b).

Besides this imaging capability, the STM can manipulate single atoms and molecules on the surface. By moving the tip closer to an adatom (adsorbed atom on surface), a partial chemical bonding forms between the outmost atom on the tip and the adatom. The adatom will then follow the tip wherever it is moved along the surface. Once the adatom has been positioned to the desired spot, it is released by pulling the tip away from the surface. Alternatively, by using a series of voltage pulses, the STM tip can act as a crane to pick up single adatoms from the

surface and put them back down. Using these techniques, complicated artificial structures can be built with atomic precision (Fig.1c).

The last powerful capability of STM is its spectroscopic capability. It is achieved by applying small modulation voltage between tip and sample and measuring corresponding modulation of tunneling current. While the dependence of current on position reveals the geometric structure of the surface, the dependence of current on voltage gives information about its electronic structure.

Instrumentation

For the last three years, we have been building up a custom STM which operates at low temperature (-260 ^{o}C) in an ultrahigh vacuum ($< 1 \times 10^{-10}$ Torr) environment(Fig.2a, b). In order to hold the tip stably within 1 nm of a surface, all electrical noise and mechanical vibrations have to be minimized. With our vibration isolation system, we achieved better than 0.002nm tunneling junction stability. The ultrahigh vacuum chamber allows us to prepare and maintain surfaces that are clean on the atomic scale. The system consists of three chambers; STM chamber, sample preparation chamber and load lock chamber. The load lock chamber is used to transfer samples and tips from the outside without breaking vacuum. The sample is then cleaned in the sample preparation chamber by repeated cycles of sputtering and annealing. Ionized Ar gas, Ar^+, is accelerated onto the sample from the sputtering gun and blasts the surface to get rid of oxide films and impurities. The sample is then annealed at high temperature usually several hundred degree (^{o}C) to smooth out the surface.

After preparation, the clean sample is transferred to the STM chamber. The low temperature operation is useful for maintaining the clean surface, and for freezing-out thermal motion of atoms on the surface. The STM is designed such that we can easily exchange tips and

samples with a robot arm called wobble stick. The sample is brought from a few cm away to the tip with a sample motor. As seen in the Fig.2c, the motor consists of a sapphire plate and six shear actuators made of piezoelectric materials. The motors operate on a 'slip-stick' principle, much like the magician's tablecloth trick, to move the sample across macroscopic distances (i.e. cm), but with nm precision. The motor is also able to move laterally so that different area of the sample can be studied.

Our instrument has unique capabilities which stem from a combination of STM and optical spectroscopy. An in-situ lens allows us to focus a laser to a 5 μm diameter spot on the tip, and collect light efficiently. To optimize the focus, we have built custom slip-stick motors which allow us to position the lens along four different axes: x, y, z and rotation. Using this unique capability, we are developing methods for tip-enhanced Raman scattering (an optical technique for measuring vibrational modes of molecules), and optical spin injection (a technique for studying spin dynamics in semiconductors).

Results and Discussion

GaAs(110) structure and the 'atom-by-atom substitution' technique

The sample used in this study is a *p*-type GaAs(100) wafer doped with 10^{18} Zn atoms per cm^{-3}. The clean GaAs(110) surface is prepared by cleaving GaAs(100) wafer inside the chamber. Depending on the bias voltage, either Ga or As atoms can be imaged with the STM. This is because at positive voltage, the STM probes atoms which contribute to the semiconductor's conduction band (i.e. Ga), while at negative voltage, the STM probes atoms which contribute to the valence band (i.e. As). Fig.3a is a typical topography image of GaAs(110) surface at -1.5V which shows As rows along the <110> direction.

Once a clean GaAs(110) is ready, a low coverage of Mn atoms is evaporated onto the surface from a home-built electron-beam evaporator (Fig.3b). To more closely mimic a bulk-like environment, single Mn atoms are then substituted for Ga in the first layer of the surface, by applying a voltage pulse with the STM tip[5].

Single Mn acceptors measured with non-magnetic tips

The electron configuration of the Mn atom is [Ar]$3d^5 4s^2$ and the five electrons in $3d$ shell align parallel and fill each of five $3d$ states according to Hund's rule. Thus the total orbital angular momentum is L=0 and it has S=5/2 spin angular momentum. The local $3d$ moments in Mn atoms hybridize and form bonding states with GaAs $4sp$ orbitals. Due to the one missing $4p$ electron in the Ga site, incorporated Mn atom provides a core S=5/2 spin and a p-like bound hole to the system as an acceptor (Fig.4a). And the local $3d$ moment and weakly bound p-like hole couple antiferromagnetically (spins are anti-parallel) due to p-d exchange interaction. The weakly bound holes are believed to mediate magnetic interactions among Mn acceptors and this long range hole-mediated interaction cause ferromagnetism in diluted ferromagnetic semiconductors[6].

The hole then occupies anti-bonding state of Mn which is 113meV above from the valence band edge. Therefore the hole now can tunnel from sample to tip when a positive bias voltage is applied and we measure Mn acceptor state from *dI/dV* spectroscopy. The spectroscopy measured on single Mn acceptors with non-magnetic Ag tips shows a strong resonance peak at 0.85V inside the band gap of *p*-GaAs whose band gap is about 1.52eV at -260 °C (Fig.4b). On the other hand, spectroscopy measurements on two nearest neighbor As atoms show enhancement in valence band which is due to *p*-*d* interactions between introduced Mn acceptor and two neighboring As atoms.

Typical STM images of single Mn acceptors are shown in Fig.4c, d which are unoccupied and occupied states of Mn acceptors. Image measured with negative bias voltage shows a dumbbell-like shape. The two bright features which are nearest neighboring As atoms of Mn acceptor are direct consequences of the valence band enhancements discussed above. On the other hand, crystal anisotropy of zinc-blende GaAs crystal structure causes star-like shapes of occupied states of Mn acceptors.

The resonance peak at 0.85V seems to be too large compared with its bulk impurity level at 113meV. This discrepancy comes from the effect so-called tip-induced band bending (TIBB). When a metal tip is located near a semiconductor, the energy band of the semiconductor is bending according to match Fermi level of tip and sample[5]. It has been well understood from the studies of planar metal-oxide-semiconductor structures. This TIBB near the surface of GaAs mainly shifts Mn acceptor level from 113meV to 850meV. However after this initial shift, TIBB doesn't cause any additional shift of peak position. It was verified from the measurements with different tunneling distances and micro-shapes of tip.

While we didn't see a further shift due to TIBB, sometimes we measured different peak positions from single Mn acceptors which are around 0.73V. It is not clearly understood yet but one possible interpretation is that positively charged subsurface Zn impurities near Mn acceptors alter local potential landscapes and cause additional band bending effects on Mn acceptor level. Recent STM studies on Mn acceptors located in a 2nd layer from a surface of bulk InMnAs also shows different peak positions ranging from 0.4 to 0.9V[7]. Therefore the additional peak shift might be understood as an effect of different local environments on Mn acceptor level and it requires further studies.

Hole-mediated spin-spin interactions: Study on Mn pairs

After the experiments on single Mn acceptors, we extend the studies to pairs of substituted Mn. By using same manipulation and substitution techniques, we could make different pairs of Mn acceptors.

For example, the Mn pair in Fig.5a is aligned along the <100> direction, with the two Mn acceptors spaced apart by 5.65Å. Spectroscopy measurements on this pair show a single resonance peak located at the same positions as one measured on single acceptors. On the other hand, measurements on a different type of Mn pair which is aligned along the <110> direction, with the Mn atoms 4Å apart shows two resonant peaks separated by about 470meV (Fig.5b).

It was previously found that pairs of Mn acceptors exhibit an exchange splitting which depends on their separation and crystal orientation[5]. For example, coupling between two Mn atoms switches from ferromagnetic (parallel spins) to antiferromagnetic (anti-parallel spins) depending on the pair's orientation.

When two Mn spins interact ferromagnetically (two spins are the same direction), the resonance peak splits into bonding and anti-bonding energy states, analogous to the formation of a hydrogen molecule. Thus, two peaks are observed in the STM measurements, with a splitting from which we can estimate the strength of ferromagnetic interaction between the Mn pair.

On the other hand, two Mn spins which interact antiferromagnetically (spins aligned in the opposite direction) can stay together in the same energy level and therefore no exchange splitting is expected in this pair. For this reason, the first Mn pair in Fig. 5a (<100> pair) can be understood as an antiferromagnetic coupled Mn pair. The different magnetic couplings observed from the pairs of different crystal orientations show an evidence of strong magnetic anisotropy in GaMnAs.

In addition to the orientation dependence, the magnetic interaction also depends on the separation distance between the atoms. A third type Mn pair along the <110> direction, but now 12Å apart was prepared for the comparison with the first pair (<110> pair and apart 4Å). While the first Mn pair exhibits two resonance peaks, the third Mn pair does not show exchange splitting (Fig.5c). This reflects either a weaker ferromagnetic interaction, or perhaps that the pair is coupled antiferromagnetically.

The STM studies on Mn pairs not only give a better microscopic understanding of hole-mediated magnetic interactions in GaMnAs but also show a future research direction in this system. The dependence of magnetic interactions on crystal orientation and separation suggests a possibility of higher ferromagnetic transition temperature, T_c in GaMnAs with better growth technique. For example, making more ferromagnetic pairs (e.g. the first type of pair) or reducing number of antiferromagnetically coupled pairs (e.g. the second and third types of pairs) are expected to enhance ferromagnetic interactions in the system. For the better understanding of this dependency, we are working on experiments on other types of Mn pairs, trimers and larger clusters. In parallel, we are also developing a capability for spin-polarized STM to better study long range magnetic coupling.

Early efforts for spin-polarized STM measurements

Spin-polarized STM (SP-STM) is nothing but a conventional STM except that now a magnetic tip is used for the measurements. However this small change causes big difference for the measurement of magnetic properties. SP-STM works by selectively detecting spin-polarized tunneling current depending on the relative orientation of tip and sample magnetization directions. Tunneling resistance between parallel magnetizations is smaller than one between

anti-parallel magnetizations. Therefore the net tunneling current measured with SP-STM gives spatial information of sample magnetization[8].

To characterize the magnetic orientation of the STM tips, we need reference samples with well known magnetization directions. We have been preparing two magnetic samples: Co nanoislands on Cu(111) and Cr(001) (Fig.6a, b). For the first sample, we evaporated Co atoms on cleaned Cu(111) at room temperature and the Co atoms form bi-layers of triangular shape of nanoislands on Cu(111) surface[9] . These islands exhibit out-of-plane magnetization and can be used to test whether SP-STM tip has a component of out-of-plane magnetization. The second sample is Cr(001) which is an antiferromagnetic sample and shows in-plane spin contrast whose magnetization is alternating along neighboring terraces[10]. It will be used to test in-plane component of magnetization of SP-STM tip.

With non-magnetic tips, we measured some characteristic features of Co nanoislands on Cu(111) and Cr(001) such as d_z surface state of Co islands at -340meV and orbital Kondo resonance of Cr(001) at -50meV (Fig.6c, d). We also tried magnetic Ni and Cr tips to see any spin contrast but so far haven't seen the expected spin-related contrast. This likely reflects the suppression of spin contrast by impurities on the surface [11] , so that better sample preparation is needed.

In preliminary STM experiments on GaAs using tips made from Ni (ferromagnet) or Cr (antiferromagnet), we try to extend the study of magnetic interactions in Mn pairs and clusters by directly detecting the different spin states. With a Ni tip, we observed two resonance peaks from 'single' Mn acceptors. It is not clear yet why two peaks appear with Ni tip but one possible interpretation is that the secondary peak might be one of two spin excited states due to spin-orbit interaction.

Conclusion

With a home-built low temperature ultrahigh vacuum STM, we measured resonance peaks from single Mn acceptors in p-GaAs. Magnetic interactions between pairs of Mn acceptors are also studied and they show separation and orientation dependent interactions. As early trials, magnetic Ni tips are used for the study of SP-STM measurements on Mn pairs.

These studies are expected to contribute to a microscopic understanding of the underlying physics of GaMnAs, and will help in the search for new semiconductor materials which exhibit ferromagnetism above room temperature.

References

[1] H. Ohno, A. Shen, F. Matsukura, A. Oiwa, A. Endo, S. Katsumoto and Y. Iye,

   Appl. Phys. Lett. **69**, 364 (1996)

[2] H. Ohno, D. Chiba, F. Matsukura, T. Omiya, E. Abe, T. Dietl, Y. Ohno and

   K. Ohtani, Nature **408**, 944 (2000)

[3] J. A. Gupta, R. Knobel, N. Samarth and D. D. Awschalom, Science **292**, 2458 (2001)

[4] A.H. Macdonald, P Shiffer and N. Samarth, Nature materials 4, 195 (2005)

[5] D. Kitchen, A. Richardella, J.M. Tang, M.E. Flatte and A. Yazdani, Nature **442**, 436 (2006)

[6] T. Jungwirth, J. Sinova, J. Masek, J. Kucera and A.H. Macdonald,

   Rev. of Mod. Phys. 78, 809 (2006)

[7] F. Marczinowski, J. Wiebe, J.M. Tang, M.E. Flatte, F. Meier, M. Morgenstern

   and R. Wiesendanger, Phys. Rev. Letts. **99**, 157202 (2007)

[8] M. Bode, Rep. Prog. Phys. **66,** 523 (2003)

[9] O. Pietzsch, A. Kubetzka, M. Bode and R. Wiesendanger,

  Phys. Rev. Letts. **92**, 057202 (2004)

[10] M. Kleiber, M. Bode, R. Ravlic, N. Tezuka and R. Wiesendanger,

  J. of Mag. and Mag. Mats., **240** 64 (2002)

[11] M. Sicot, O. Kurnosikov, O.A.O. Adam, H.J.M. Swagten and B. Koopmans,

  Phys. Rev. B. **77**, 035417 (2008)

[12] This structure was built by my advisor Dr. Jay Gupta when he was a Post Doc. at IBM
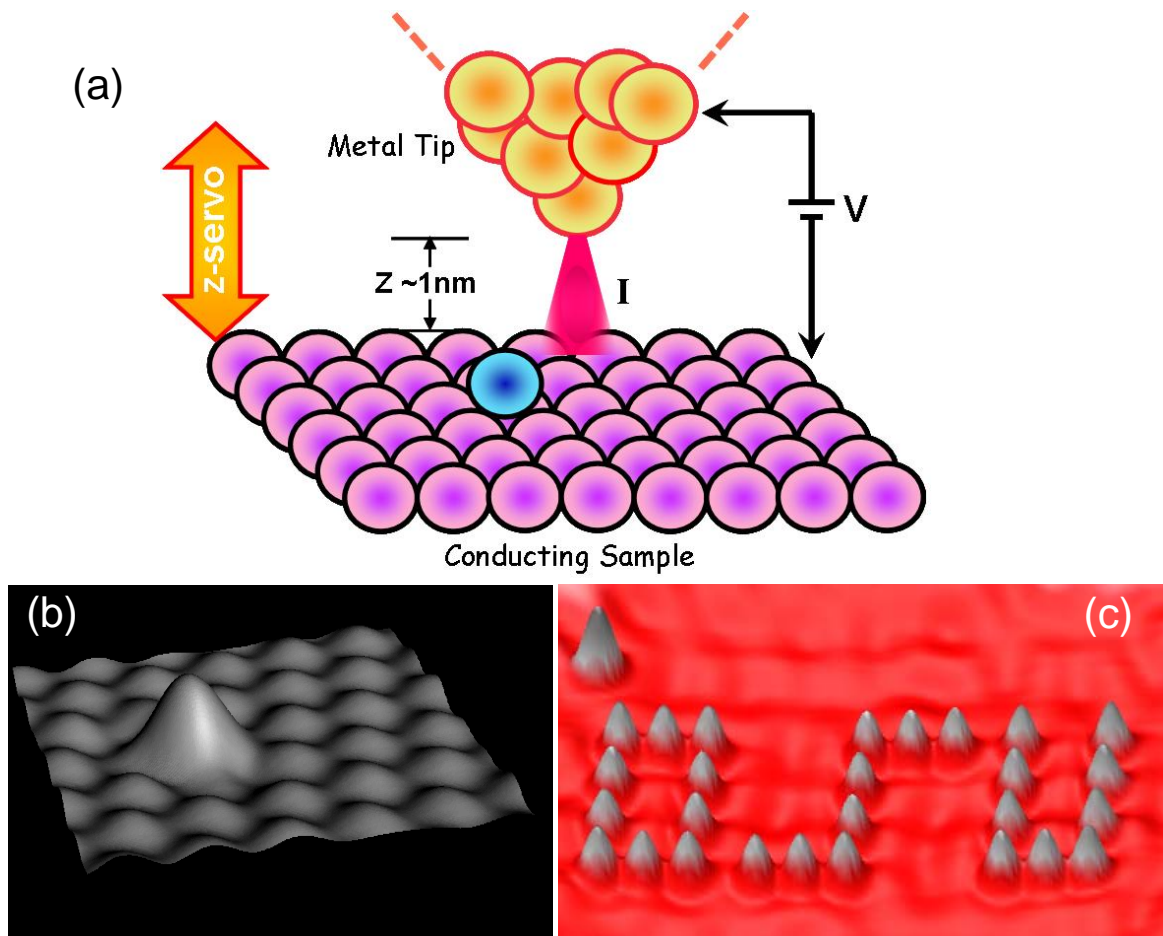
Almaden research center.

Fig. 1 (a) Schematic drawing of STM tunneling junction (b) STM image of single Pt adatom on Pt(111) surface (c) The Ohio State University logo built with 27 Co adatoms on Cu(111) surface[12]
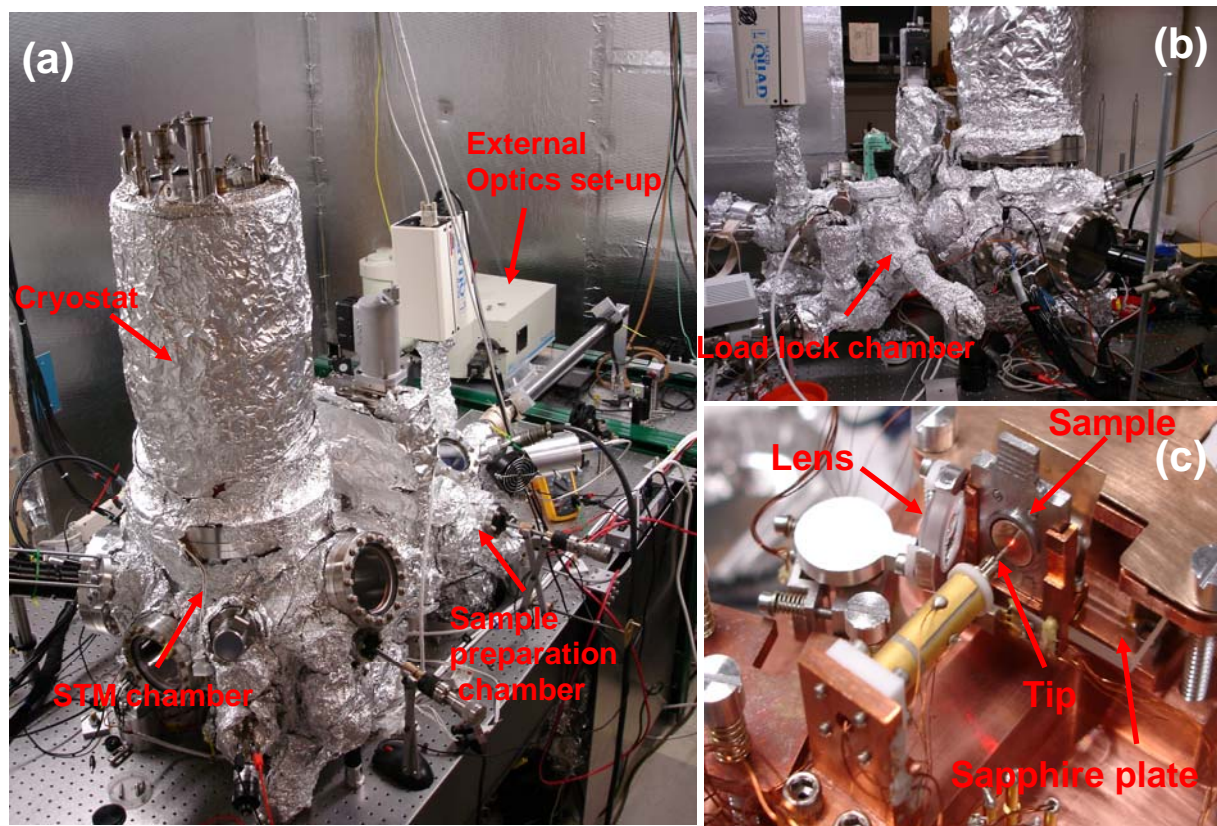
Fig.2 (a), (b) External views of a home-built low temperature, ultrahigh vacuum scanning tunneling microscope. STM is located inside of light and sound tight acoustic room. Three main chambers and a cryostat which has liquid He and Nitrogen baths are shown. STM chambers are mounted on an optical table where external optics set-ups are prepared such as mirrors, lens, filters, CCD camera, photospectrometer and so on. (c) Close view of STM tunneling junction. Tip, sample and in-situ lens are shown. Lens and sample are controlled by 'slip-stick' coarse approach motors. Tip is mounted in piezoelectric tube which is used to scan tip over the surface of sample and feedback control tunneling distance.
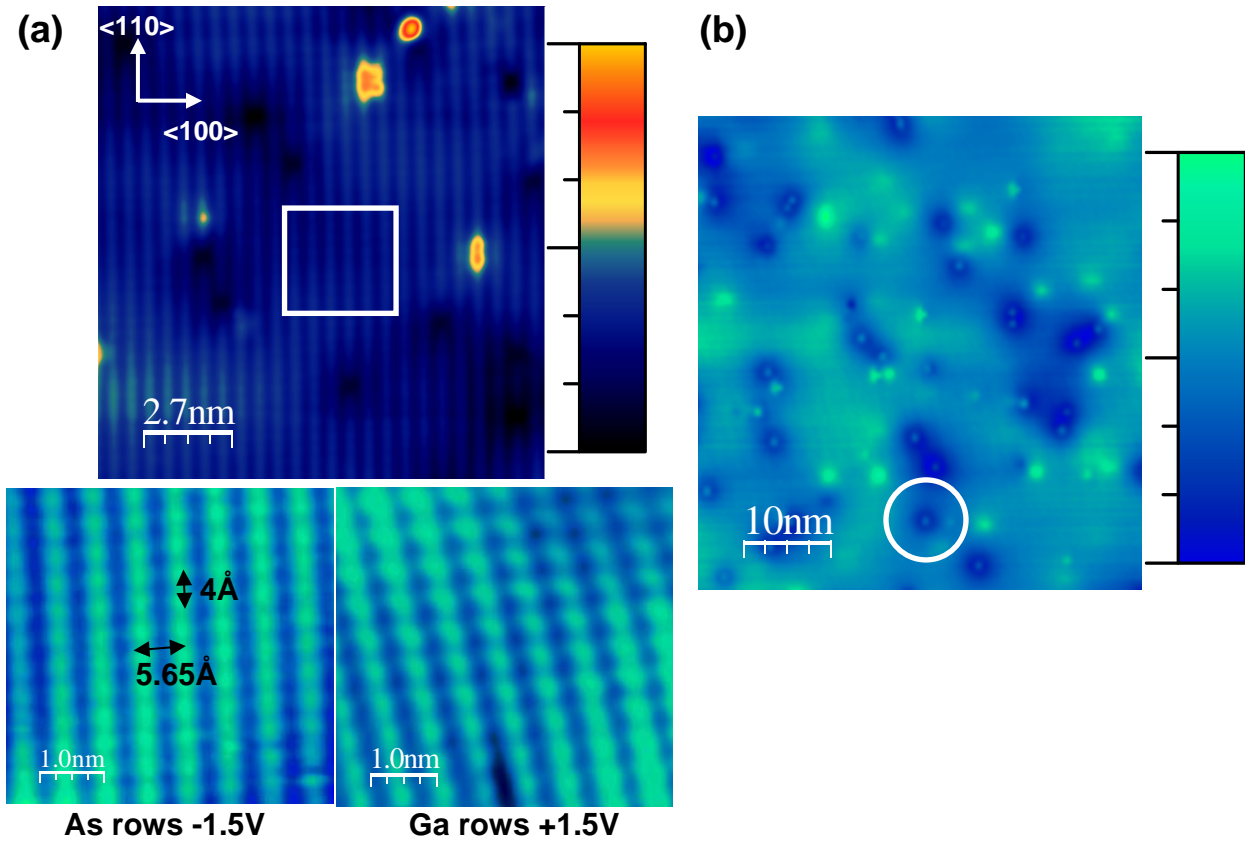
(a) <110>
<100>
2.7nm
↕ 4Å
↔ 5.65Å
1.0nm
1.0nm
As rows -1.5V
Ga rows +1.5V

(b) 10nm

Fig.3 (a) Topography image of cleaved *p*-GaAs(110) surface at -1.5V bias voltage and 0.7nA tunneling current. Lower two images are zoom in images of rectangular box in the upper image. Equally spacing As and Ga rows are shown depending on the polarity of a bias voltage.

(b) Low coverage of Mn single atoms are evaporated onto a cold GaAs(110) sample from a custom electron-beam evaporator. Circular shape of Mn adatoms are shown on cleaved p-GaAs(110) surface at -0.7V bias voltage and 0.3nA tunneling current.
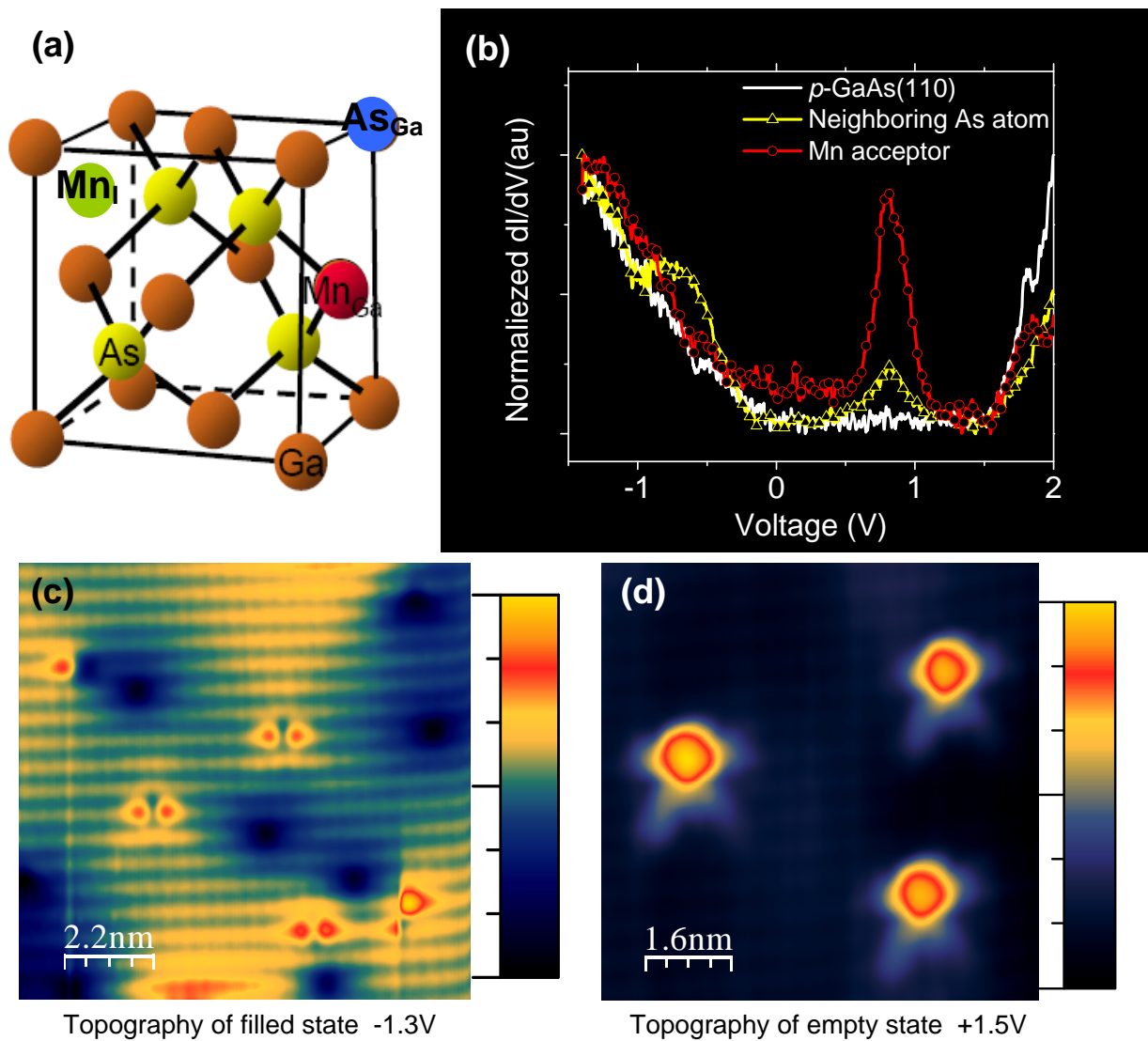
Fig.4 (a) Schematic drawing for GaAs's zinc-blende crystal structure. Mn atoms are incorporated into Ga sites and become Mn^{2+} acceptor while providing one bound hole. (b) Spectroscopy on single Mn acceptor shows a strong in-gap resonance peak around 0.85V. On the other hand, spectroscopy on two nearest neighboring As atoms shows valence band enhancement at negative bias voltage. (c) Dumbbell-shapes of three single Mn acceptors are shown at negative bias voltage. (d) Star-shapes of single Mn acceptors at positive bias are due to crystal anisotropy structure of GaAs host sample.
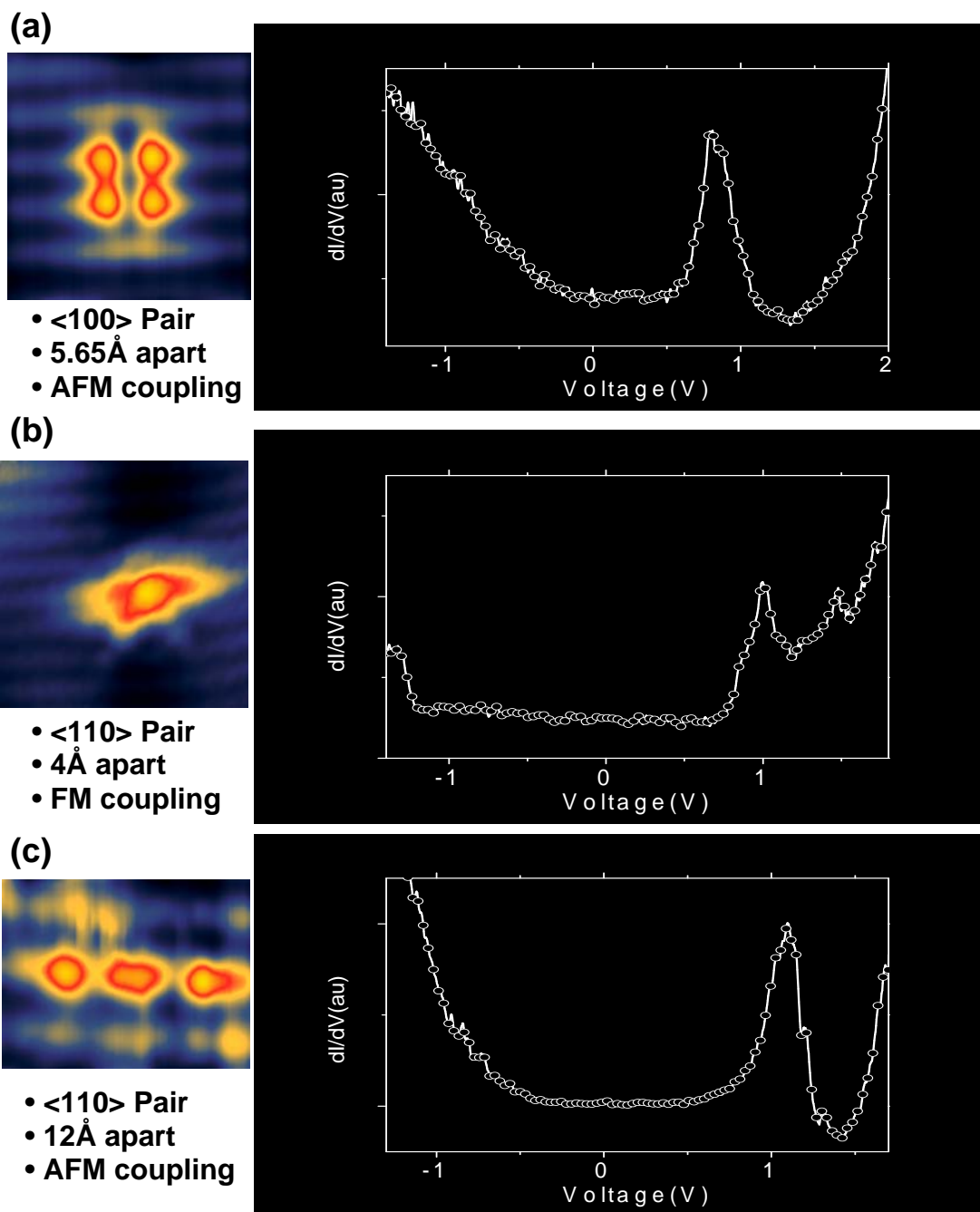
Fig. 5 (a) <100> Mn pair shows no exchange splitting (antiferromagnetically coupled). (b)

<110> Mn pair separated by 4Å shows ferromagnetic coupling with 470meV energy splitting.

(c) <110> Mn pair separated by 12Å shows antiferromagnetic coupling.

(a) Topography 0.8v, 0.7nA

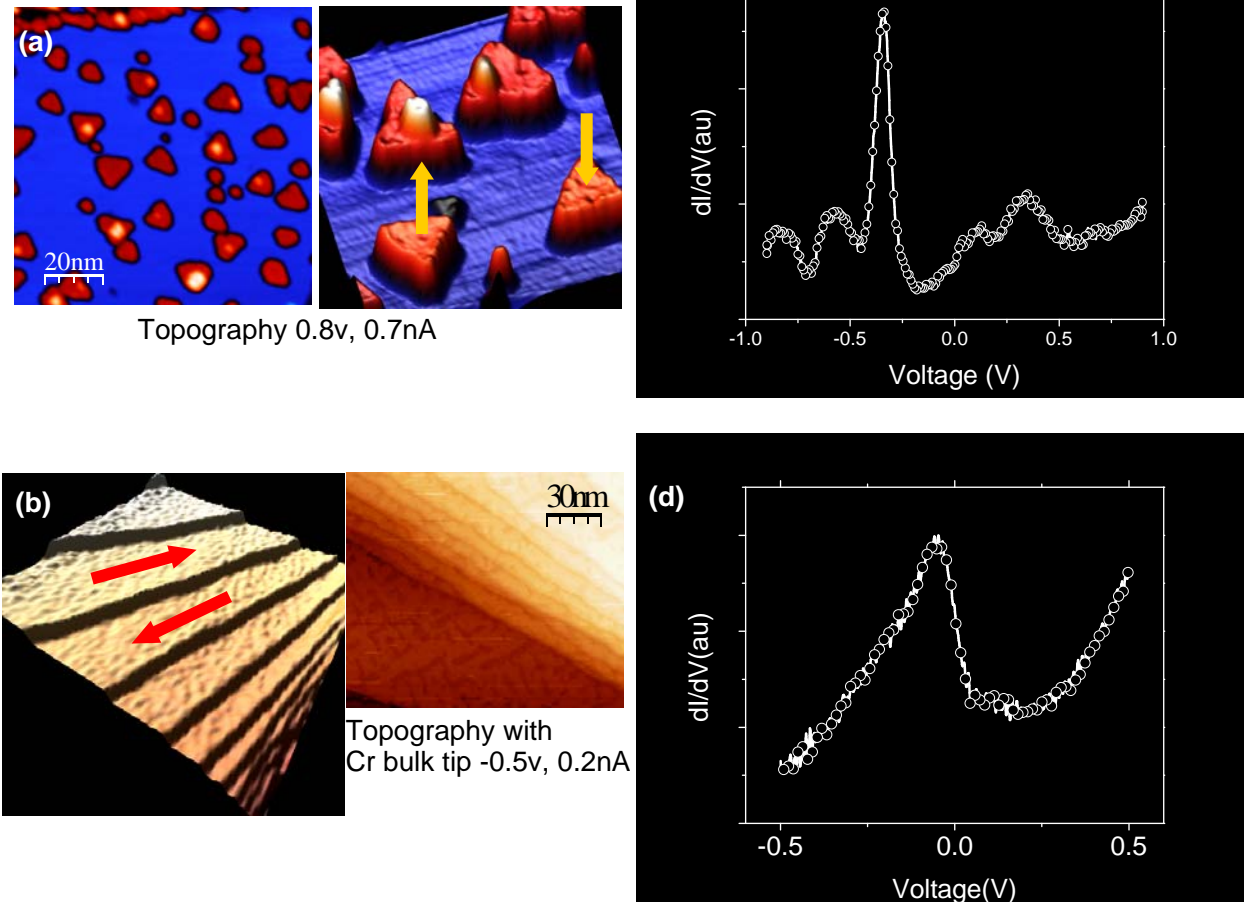**(b)** Topography with Cr bulk tip -0.5v, 0.2nA

(c)

(d)

Fig. 6 (a) Triangular shape of Co nanoislands on Cu(111) surface. Yellow arrows indicate out-of-plane magnetization directions. (b) Antiferromagnetic Cr(001) sample exhibits in-plane magnetization (red arrows). Segregated C, N and O impurities are shown in the images. (c) With non-magnetic PtIr tip, we measured minority d_{z2} surface state at -0.34V and free electron state at +0.35V from the Co nanoislands on Cu(111). (d) Orbital Kondo resonance of $d_{xz,yz}$ surface state is observed at -50mV with non-magnetic Au tip.